*Int. J. Heat Mass Transfer*. Vol. 34, No. 7, pp. 1905–1908, 1991
Printed in Great Britain

0017-9310/91 \$3.00+0.00


# Turbulent Prandtl number in the near-wall region of a turbulent channel flow

R. A. ANTONIA
Department of Mechanical Engineering, University of Newcastle, N.S.W., 2308, Australia

and

J. KIM
Center for Turbulence Research, NASA–Ames Research Center, Moffett Field, CA 94035, U.S.A.

(*Received* 18 *May* 1990 *and in final form* 10 *August* 1990)

A SIGNIFICANT amount of effort has been devoted to the determination of the turbulent Prandtl number $Pr_T$ in turbulent wall shear flows (e.g. ref. [1]). Nonetheless, reliable trends for the dependence of $Pr_T$ on the distance from the wall and/or the molecular Prandtl number $Pr$ have yet to emerge, especially for the near-wall region where measurements are extremely difficult [2]. Reliable near-wall values of $Pr_T$ should be important in guiding the development of turbulence models which aim to calculate the heat transport near the wall.

The availability of direct numerical simulations (DNS) has enabled turbulence quantities in the near-wall region to be determined more accurately than has been hitherto possible experimentally. DNS data for the velocity field in a turbulent channel flow were recently extended to the scalar field. Starting with a fully developed velocity field, simulations were carried out for a passive scalar for three values of $Pr$ [3, 4]. The results of this simulation enable near-wall distributions of the turbulent Prandtl number and its dependence on $Pr$ to be examined. An assumption which is usually made (e.g. ref. [5]) in the context of deriving the mean temperature profile in the wall region is that the thermal eddy diffusivity does not depend on $Pr$. The results of this note indicate that only the first-order terms in the Taylor series expansions for the eddy diffusivity and the turbulent Prandtl number are independent of $Pr$, at least to a first approximation. Also examined are the near-wall behaviour of the correlations between the temperature fluctuation $\theta$ and the velocity fluctuations $u$ and $v$ as well as their dependence on $Pr$.

For the simulations considered here (case I in refs. [3, 4]) the initial and boundary conditions on the instantaneous temperature $T$ are

$$T(x, y, z, t = 0) = \frac{y}{h}\left(1 - \frac{y}{2h}\right)$$

$$\left.\begin{matrix} T(x, y = 0, z, t) \\ T(x, y = 2h, z, t) \end{matrix}\right\} = 0$$

the walls being located at $y = 0$ and $2h$. A constant source term is used for each scalar field so that the scalar is created internally and removed at both walls.

In this flow, the mean temperature $\bar{T}$ satisfies the equation

$$\frac{\partial}{\partial y^+}\overline{v^+\theta^+} = \frac{1}{Pr}\frac{\partial^2 \bar{T}^+}{\partial y^{+2}} + \frac{Q_i}{h^+} \tag{1}$$

where $Q_i$ is the non-dimensional source term, equal to 1 since $Pr^{-1}\,\partial\bar{T}^+/\partial y^+$ is equal to 1 at $y^+ = 0$. Integration of equation (1) yields

$$-\overline{v^+\theta^+} + \frac{1}{Pr}\frac{\partial \bar{T}^+}{\partial y^+} = 1 - \frac{y^+}{h^+}. \tag{2}$$

The linear variation across the duct of the total heat flux is therefore analogous to the linear distribution of the total shear stress

$$-\overline{u^+v^+} + \frac{\partial \bar{U}^+}{\partial y^+} = 1 - \frac{y^+}{h^+}. \tag{3}$$

Taylor series expansions of $\overline{u^+v^+}$, $\overline{v^+\theta^+}$, $\bar{U}^+$, $\bar{T}^+$, away from $y^+ = 0$, are

$$\overline{u^+v^+} = \alpha_1 y^{+3} + \beta_1 y^{+4} + \gamma_1 y^{+5} \tag{4a}$$

$$\overline{v^+\theta^+} = \alpha_2 y^{+3} + \beta_2 y^{+4} + \gamma_2 y^{+5} \tag{4b}$$

$$\bar{U}^+ = y^+ - \frac{1}{2h^+}y^{+2} + d_1 y^{+4} + e_1 y^{+5} \tag{4c}$$

$$\bar{T}^+ = Pr\,y^+ - \frac{Pr}{2h^+}y^{+2} + d_2 y^{+4} + e_2 y^{+5} \tag{4d}$$

with terms up to order five retained. Except for the quadratic terms in $\bar{U}^+$ and $\bar{T}^+$, these expressions are identical to those given in ref. [6] for a zero pressure gradient turbulent boundary layer. Overbars in equations (2)–(4) denote averaged values. Averaging was carried out over a non-dimensional period $t^+ \equiv tU_\tau^2/\nu$ equal to about 500 after the flow field had reached a steady state. Averaging was also carried out over the $128 \times 128$ grid points in the $x$- and $z$-directions. The effective averaging time was sufficient to ensure convergence of all the averaged quantities presented here.

It has been argued [5, 7] that the coefficients $\alpha_2$, $\beta_2$, $\gamma_2$ should not depend on $Pr$. Kader [7] assumed that the eddy diffusivity is determined only by velocity and temperature fluctuations and cannot therefore depend on $Pr$. This assumption does not however appear to be supported either by experiments [1] or models [8]. It would seem reasonable to expect that the coefficients in $\overline{v^+\theta^+}$ like those in $\bar{T}^+$ should, in general, depend on $Pr$. Distributions for $\overline{v^+\theta^+}$ and $\bar{T}^+$ are shown in Figs. 1 and 2, respectively. The ratios $\overline{v^+\theta^+}/y^{+3}$ and $\bar{T}^+/y^+$ have been plotted mainly to highlight the behaviour of the leading order terms in equations (4b) and (4d). A logarithmic scale has been used for the abscissa to emphasize the near-wall region while still allowing the behaviour of the data to be viewed up to $y = h$. For comparison, distributions of $\overline{u^+v^+}/y^{+3}$ are also shown in Figs. 1 and 2. Figure 1 shows that $\alpha_2$ increases with $Pr$. This increase is however approximately linear, the ratio $\alpha_2/Pr$ being roughly constant (Table 1). Figure 2 shows, as expected, that as $y^+ \to 0$, $\bar{T}^+/y^+$ approaches a constant value equal to $Pr$. The extent of the plateau increases as $Pr$ decreases. The tabulated values of the coefficients were obtained from least squares fits to data in the region $0 < y^+ \leqslant 5$.

Substitution of expressions (4) into equations (2) and (3) yields the following relations between some of the coefficients in expressions (4)

## NOMENCLATURE

- $d_i, e_i$ coefficients in equations (4)
- $h$ half-width of channel
- $Pr$ molecular Prandtl number, $\nu/\gamma$
- $Pr_T$ turbulent Prandtl number, equation (6)
- $Q_i$ constant source term, equation (1)
- $Q_w$ thermometric wall heat flux
- $T, \bar{T}$ instantaneous and mean temperature
- $T_w$ wall temperature
- $T_\tau$ friction temperature, $Q_w/U_\tau$
- $\bar{T}^+$ $(\bar{T}_w - \bar{T})/T_\tau$
- $\bar{U}$ mean velocity in the $x$-direction
- $U_\tau$ friction velocity, $\tau_w^{1/2}$
- $u, v, w$ velocity fluctuations in the $x$-, $y$-, $z$-directions, respectively
- $-\overline{uv}$ Reynolds shear stress
- $\overline{v\theta}$ turbulent heat flux
- $x, y, z$ coordinates in the streamwise, normal and spanwise directions, respectively.

Greek symbols

- $\alpha_i, \beta_i, \gamma_i$ coefficients in equations (4), (10), (11) and (13)
- $\gamma$ thermal diffusivity
- $\theta$ temperature fluctuation
- $\nu$ kinematic viscosity
- $\rho_{uv}$ correlation coefficient, $\overline{uv}/u'v'$
- $\rho_{u\theta}$ correlation coefficient, $\overline{u\theta}/u'\theta'$
- $\rho_{v\theta}$ correlation coefficient, $\overline{v\theta}/v'\theta'$
- $\tau_w$ kinematic wall shear stress.

Subscript

- w wall value.

Superscripts

- $+$ normalization by $U_\tau$ for velocity, $T_\tau$ for temperature and $\nu/U_\tau$ for a length scale
- $'$ r.m.s. quantity, e.g. $u' \equiv (\overline{u^2})^{1/2}$.

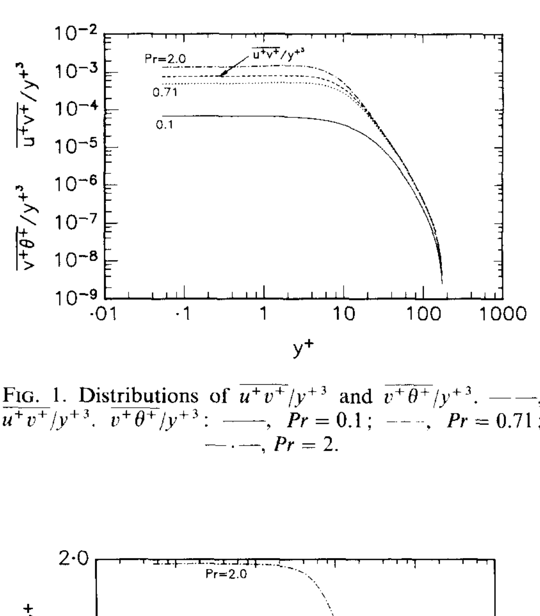


FIG. 1. Distributions of $\overline{u^+v^+}/y^{+3}$ and $\overline{v^+\theta^+}/y^{+3}$. ——, $\overline{u^+v^+}/y^{+3}$. $\overline{v^+\theta^+}/y^{+3}$: ——, $Pr = 0.1$; – – –, $Pr = 0.71$; —·—, $Pr = 2$.

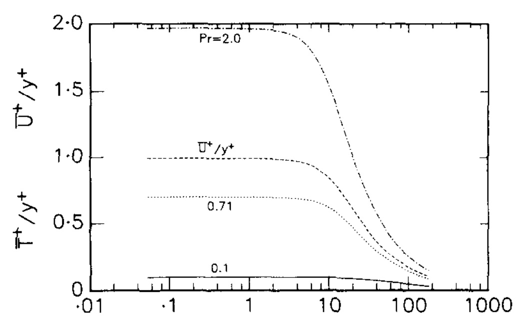


FIG. 2. Distributions of $\bar{U}^+/y^+$ and $\bar{T}^+/y^+$. ——, $\bar{U}^+/y^+$. $\bar{T}^+/y^+$: ——, $Pr = 0.1$; – – –, $Pr = 0.71$; —·—, $Pr = 2$.

$$\alpha_1 = 4d_1, \quad \alpha_2 = \frac{4d_2}{Pr}, \quad \beta_1 = 5e_1, \quad \beta_2 = \frac{5e_2}{Pr}. \tag{5}$$

At $y^+ = 0$, $Pr_T$ is given by

$$Pr_T = \frac{\overline{u^+v^+}\,(\mathrm{d}\bar{T}^+/\mathrm{d}y^+)}{\overline{v^+\theta^+}\,(\mathrm{d}\bar{U}^+/\mathrm{d}y^+)} = \frac{\alpha_1}{\alpha_2}Pr = \frac{d_1}{d_2}Pr^2. \tag{6}$$

Since $\alpha_2 \sim Pr$ (or alternatively $d_2 \sim Pr^2$), equation (6) implies that, as $y^+ \to 0$, $Pr_T$ should be constant, independent of $Pr$, to a reasonable approximation. The distributions in Fig. 3 show that this is indeed the case. (The present value of $\alpha_1$ is $7.48 \times 10^{-4}$, in close agreement with that given in Mansour *et al.* [9].) The wall value of $Pr_T$ reported in ref. [6] (for $Pr = 0.73$) is approximately 60% smaller than the present value due to an over-estimation of $\alpha_2$, which was deduced from $d_2$ using the second relation in equation (5). Kader [7] assumed that all the coefficients in the expansion for the eddy diffusivity were independent of $Pr$. This leads to a $Pr^2$ dependence for $d_2$ and $e_2$. While the present data support a $Pr^2$ dependence for $d_2$, a definite statement cannot be made with respect to $e_2$. Although values of $\beta_2$ $(= 5e_2/Pr)$ were computed, they are not sufficiently accurate to draw conclusions about any $Pr$ dependence for $e_2$. Cebeci's [8] conclusion, based on a Stokes-type flow model, that, at the wall, $Pr_T$ depends strongly on $Pr$ and becomes constant (independent of $Pr$) away from the wall, is the opposite of the trend in Fig. 3. Away from the wall, Fig. 3 suggests that the dependence of $Pr_T$ on $Pr$ should be relatively weak for $Pr \gtrsim 1$, the $Pr_T$ distributions for $Pr = 0.71$ and 2.0 following each other closely. This seems to be in accord with the observation of Jischa and Rieke [10].

An indirect, but interesting from a physical point of view, way of estimating $Pr_T$ at $y^+ = 0$ was suggested by Orlando *et al.* [11]. The suggestion was based on the assumption that there is a perfect correlation between $u$ and $\theta$ at $y^+ = 0$, namely

$$\rho_{u\theta} = \frac{\overline{u\theta}}{u'\theta'} = 1. \tag{7}$$

Table 1. Values of coefficients $\alpha_i$ in correlations containing $\theta$

| $Pr$ | $\alpha_2$ | $\alpha_2/Pr$ | $\alpha_4$ | $\alpha_4/Pr$ | $\alpha_5$ | $\alpha_5/Pr$ |
|---|---|---|---|---|---|---|
| 2 | $1.358 \times 10^{-3}$ | $6.79 \times 10^{-4}$ | 0.746 | 0.373 | 0.248 | 0.124 |
| 0.71 | $4.795 \times 10^{-4}$ | $6.75 \times 10^{-4}$ | 0.255 | 0.359 | $8.642 \times 10^{-2}$ | 0.122 |
| 0.1 | $6.744 \times 10^{-5}$ | $6.74 \times 10^{-4}$ | $2.65 \times 10^{-2}$ | 0.265 | $5.226 \times 10^{-3}$ | 0.052 |

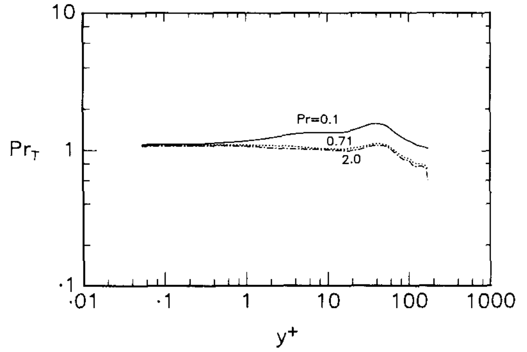


FIG. 3. Distributions of the turbulent Prandtl number: ——, $Pr = 0.1$; ---, $Pr = 0.71$; —·—, $Pr = 2$.

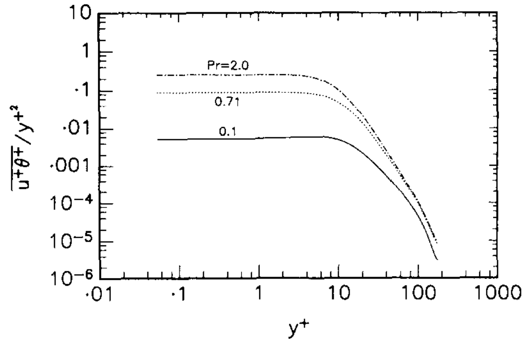


FIG. 5. Distributions of $\overline{u^+\theta^+}/y^{+2}$: ——, $Pr = 0.1$; ---, $Pr = 0.71$; —·—, $Pr = 2$.

It follows that, at $y^+ = 0$

$$\rho_{uv} = \rho_{\theta v} \tag{8}$$

and

$$Pr_T = \frac{u'^+}{\theta'^+} Pr. \tag{9}$$

The near-wall expansions for $u'^+$ and $\theta'^+$ are

$$u'^+ = \alpha_3 y^+ + \beta_3 y^{+2} + \gamma_3 y^{+3} \tag{10}$$

$$\theta'^+ = \alpha_4 y^+ + \beta_4 y^{+3} \tag{11}$$

with terms up to order three retained. (There is no $y^{+2}$ term in $\theta'^+$ as $\partial^2\theta/\partial y^2$ is zero at the wall.) At $y^+ = 0$, expression (9) becomes

$$Pr_T = \frac{\alpha_3}{\alpha_4} Pr. \tag{12}$$

For consistency with equation (6), $\alpha_4$ should increase linearly with $Pr$. The dependence of $\alpha_4$ on $Pr$ is illustrated in Fig. 4 where the ratio $\theta'^+/y^+$ is plotted against $y^+$. The value of $\alpha_3$ ($\approx 0.367$) can be inferred from the near-wall variation of $u'^+/y^+$, also shown in Fig. 4. Table 1 shows that $\alpha_4/Pr$ is approximately constant for $Pr = 0.71$ and 2. This value is in good agreement with that inferred from the boundary layer experiments ($Pr = 0.73$) of ref. [12] or the DNS data ($Pr = 1$) of ref. [13]. The numerical value of $Pr_T$ obtained from equation (12) is in agreement with that given by equation (6) for $Pr = 0.71$. This is not surprising in view of the support for equation (7), from experiments [14] and simulations [3, 4]. The expansion, away from $y^+ = 0$, for $\overline{u^+\theta^+}$ is (to third order)

$$\overline{u^+\theta^+} = \alpha_5 y^{+2} + \beta_5 y^{+3}. \tag{13}$$

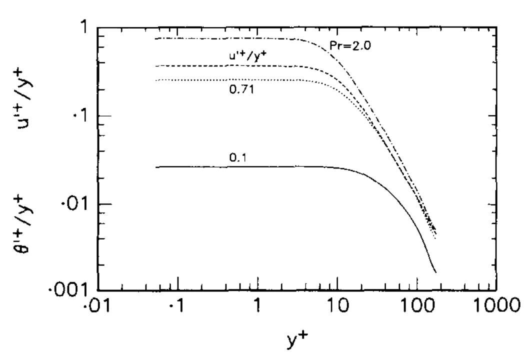


FIG. 4. Distributions of $u'^+/y^+$ and $\theta'^+/y^+$. — —, $u'^+/y^+$. $\theta'^+/y^+$: ——, $Pr = 0.1$; ---, $Pr = 0.71$; —·—, $Pr = 2$.

Table 2. Wall values of turbulent Prandtl number and correlation coefficients $\rho_{u\theta}$ and $\rho_{v\theta}$

| $Pr$ | $Pr_T$ Best fit | $Pr_T$ Equation (6) | $Pr_T$ Equation (12) | $\rho_{u\theta}$ Equation (14) | $\rho_{v\theta}$ Equation (15) |
|---|---|---|---|---|---|
| 2 | 1.093 | 1.102 | 0.984 | 0.906 | 0.209 |
| 0.71 | 1.103 | 1.108 | 1.022 | 0.923 | 0.216 |
| 0.1 | 1.107 | 1.109 | 1.385 | 0.537 | 0.292 |

The dependence of $\alpha_5$ on $Pr$ can be ascertained from Fig. 5 and Table 1. At $y^+ = 0$, the value of $\rho_{u\theta}$ is

$$\rho_{u\theta} = \frac{\alpha_5}{\alpha_3\alpha_4}. \tag{14}$$

The values of $\rho_{u\theta}$ in Table 2 indicate that its magnitude is indeed close to unity for $Pr = 0.71$ and 2. The DNS data ($Pr = 1$) of Lyons *et al.* [15] indicate a maximum value of 0.95 for $\rho_{u\theta}$ at $y^+ \approx 7$. Table 2 shows that $\rho_{u\theta}$ is significantly smaller ($\approx 0.54$) at $Pr = 0.1$. For small $Pr$, it would seem that equation (12) is not as good an approximation for the wall value of $Pr_T$ as equation (6). Speculatively, when $Pr \gg 1$ or $Pr \ll 1$, one may expect that temperature is not as good a marker of the near-wall organization (in this case low-speed and high-speed streaks) as for $Pr \approx 1$. For $Pr \ll 1$, a significant reduction of $\rho_{u\theta}$ would seem reasonable if $\theta$ marks a relatively large flow region. Arguably, a reduction in $\rho_{u\theta}$ may occur at $Pr \gg 1$ given that the thickness of the conductive sublayer is much smaller than the viscous sublayer so that $\theta$ becomes strictly a 'wall' marker.

For completeness, wall values of $\rho_{v\theta}$ given by

$$\rho_{v\theta} = \frac{\alpha_2}{\alpha_6\alpha_4} \tag{15}$$

where $\alpha_6$ ($= 8.7 \times 10^{-3}$) is the first term in the expansion of $v'^+/y^{+2}$ near the wall, are included in Table 2. For $Pr = 0.71$ and 2 they are equal ($\approx 0.21$), this value being close to $\rho_{uv}$. There is however an increase of about 38% at $Pr = 0.1$. This is consistent with the decrease in $\rho_{u\theta}$ at $Pr = 0.1$ since $\theta$ is presumably correlated with $v$ at larger distances from the wall than at higher $Pr$.

The use of near-wall DNS data for the Reynolds shear stress and heat flux indicates that the wall value of the turbulent Prandtl number is about 1.1, independent of the molecular Prandtl number. The assumption of a perfect correlation, near the wall, between the longitudinal velocity fluctuation and the temperature fluctuation yields approximately the same wall value of $Pr_T$ for $Pr = 0.71$ and 2 but becomes inaccurate at smaller (and probably much larger) values of $Pr$.

*Acknowledgement*—RAA acknowledges the support of the Australian Research Council and the Center of Turbulence Research.

## REFERENCES

1. A. J. Reynolds, The prediction of turbulent Prandtl and Schmidt numbers, *Int. J. Heat Mass Transfer* **18,** 1055–1069 (1975).
2. B. E. Launder, Heat and mass transport. In *Topics in Applied Physics*, Vol. 12: *Turbulence* (Edited by P. Bradshaw), pp. 231–287. Springer, Berlin (1976).
3. J. Kim, Investigation of heat and momentum transport in turbulent flows via numerical simulations. In *Transport Phenomena in Turbulent Flows* (Edited by M. Hirata and N. Kasagi), pp. 715–730. Hemisphere, New York (1988).
4. J. Kim and P. Moin, Transport of passive scalars in a turbulent channel flow. In *Turbulent Shear Flows 6*, pp. 35–96. Springer, Berlin (1989).
5. A. M. Yaglom, Similarity laws for constant-pressure and pressure-gradient turbulent wall flows, *Ann. Rev. Fluid Mech.* **11,** 505–540 (1979).
6. R. A. Antonia, Behaviour of the turbulent Prandtl number near the wall, *Int. J. Heat Mass Transfer* **23,** 906–908 (1980).
7. B. A. Kader, Temperature and concentration profiles in fully turbulent boundary layers, *Int. J. Heat Mass Transfer* **24,** 1541–1544 (1981).
8. T. Cebeci, A model for eddy conductivity and turbulent Prandtl number, *J. Heat Transfer* **95,** 227–234 (1973).
9. N. N. Mansour, J. Kim and P. Moin, Reynolds-stress and dissipation-rate budgets in a turbulent channel flow, *J. Fluid Mech.* **194,** 15–44 (1988).
10. M. Jischa and H. B. Rieke, About the prediction of turbulent Prandtl and Schmidt numbers, *Int. J. Heat Mass Transfer* **22,** 1547–1555 (1979).
11. A. F. Orlando, R. J. Moffat and W. M. Kays, Turbulent transport of heat and momentum in a boundary layer subject to deceleration, suction and variable wall temperature, Report HMT-17, Thermosciences Division, Department of Mechanical Engineering, Stanford University (1974).
12. L. V. Krishnamoorthy and R. A. Antonia, Temperature-dissipation measurements in a turbulent boundary layer, *J. Fluid Mech.* **176,** 265–281 (1987).
13. S. L. Lyons, A direct numerical simulation of fully developed turbulent channel flow with heat transfer, Ph.D. Thesis, University of Illinois at Urbana/Champaign (1989).
14. R. A. Antonia, L. V. Krishnamoorthy and L. Fulachier, Correlation between the longitudinal velocity fluctuation and temperature fluctuation in the near-wall region of a turbulent boundary layer, *Int. J. Heat Mass Transfer* **31,** 723–730 (1988).
15. S. L. Lyons, T. J. Hanratty and J. B. McLaughlin, Direct numerical simulation of passive heat transfer in a turbulent channel flow, *Int. J. Heat Mass Transfer* **34,** 1149–1161 (1991).